Journal of Electrical Engineering & Technology (2023) 18:1419–1427
https://doi.org/10.1007/s42835-022-01344-4

ORIGINAL ARTICLE

Electrical Conductivity Evaluation Techniques for Superalloy Single-Crystal Steel

Jeon-Hong Kang[1] · Kwang Min Yu[1] · Sang Hwa Lee[1] · Seung Hoon Nahm[1] · Jae Yeong Park[1]

Received: 15 September 2022 / Revised: 10 November 2022 / Accepted: 17 November 2022 / Published online: 28 January 2023

Abstract
Superalloy single-crystal steel grade is a material for high-temperature gas turbine parts and is essential for preventing explosion accidents caused by high temperature and heat. To establish an infrastructure and a database for the characterization of gas turbine core materials, tests for thermal, mechanical, and electrical properties are required. The required thermal property tests include thermal conductivity, specific heat, and thermal expansion coefficient tests. The mechanical tests include tensile tests at room and high temperature and fatigue tests. The electrical tests include conductivity tests; also, in this study, various measurement methods were used to compare and evaluate the reliability of the evaluation results for the conductivity test. The conductivity was compared and evaluated using five methods, namely, the four-terminal, direct current comparator resistance bridge, four-point probe, van der Pauw, and eddy current. The conductivity obtained was 1.210% International Annealed Copper Standard (IACS), and the measured values for the five methods agreed with each other within 0.1% or less, with a measurement uncertainty of about 0.2% to 0.6% or less within a 95% confidence level.

Keywords Four-point probe method · Electrical resistivity · Van der Pauw method · Eddy current method

1 Introduction

Various companies are providing policy support for the establishment of a material properties database (DB) for a gas turbine design, led by their governments (General Electric in the US, Siemens in Germany, Mitsubishi in Japan, and Ansaldo Energia in Italy). Also, it is difficult to secure the core and source technologies because gas turbine power generation system technologies are secured by the governments and technology leaks are strictly controlled by the government. Korea's gas turbine base is inferior to those of advanced original equipment manufacturers, and research is conducted under the government's lead, as it takes a huge investment to establish a DB of gas turbine material properties, which is a country's core basic asset [1].

To strengthen Korea's energy technology competitiveness, the development of high-efficiency and large-capacity gas turbine engines must be continuously promoted, and for this, a DB for the design of gas turbine core parts is required. For the development of a 270 MW class (H class) gas turbine, a single-crystal superalloy material capable of withstanding 1600 °C (metal temperature: 1100 °C) or higher is essential. This material is selected for development with consideration to cast-ability, weld-ability, economic feasibility, material supply and demand, and thermomechanical characteristics. For the stable and efficient operation of gas turbine engines, it is essential to establish a DB of mechanical properties such as tension, creep, low-cycle and high-cycle fatigue of gas turbine component materials at high-temperature, and environmental resistance properties such as high-temperature cyclic oxidation. In addition, basic thermal properties such as thermal conductivity, specific heat, and thermal expansion, which are essential for optimizing gas turbine design and structural integrity, and electrical properties such as resistivity and conductivity are required. In this study, we tried to obtain the electrical properties necessary for building a material property DB of core materials required for the entire cycle, from the design of gas turbines for power generation and aviation to maintenance/repair/service during operation. We evaluated the property using five methods and presented partly in an international conference and the details are described in the content [2].

✉ Seung Hoon Nahm
shnahm@kriss.re.kr

[1] Korea Research Institute of Standards and Science (KRISS), 267 Gajeong-Ro, Yuseong-Gu, Daejeon 34113, Republic of Korea

2 Measurement Method

2.1 Materials

Ni-based super-alloy is a material widely used for blades of gas turbines for power generation, cogeneration, and aviation; It is often produced as a single-crystal or one-way solidification. To improve efficiency and performance, the operating temperature of gas turbines is gradually increasing to 1600 °C or higher, and the metallic material in the environment for this use is known to be at a temperature of 1100 °C or higher. For this study, a single-crystal Ni-alloy material slab supplied by Precision Castparts Corporation, USA (dimensions 100 mm(width) × 150 mm(length) × 20 m m(thickness)), was used.

2.2 Four-Terminal Resistance Measurement Method

The four-terminal resistance measurement method is a method to know the resistance of the sample by supplying current to both ends of the sample and measuring the potential difference between them. The resistivity (ρ) of the metal is defined as the electrical resistance against the cross-sectional area (A) and the length (L) of the sample and is obtained by the following Eq. (1) [3].

$$\rho = R\frac{A}{L}[\Omega \cdot \mathrm{m}] \tag{1}$$

where ρ is resistivity, R is the resistance to electrode spacing L, A is the cross-sectional area, and the electrical conductivity (σ) is obtained by the following Eq. (2):

$$\sigma = \frac{1}{\rho}[S/\mathrm{m}] \tag{2}$$

where the electrical conductivity (σ) is expressed in % IACS, which is a percentage unit calculated by Eq. (3) against pure copper (100% IACS). The ρ value of pure copper that was applied here is 1.7241 μΩ·cm at 20 °C.

$$\%IACS = (1/\rho) \times 1.7241\mu\Omega\ \mathrm{cm} \tag{3}$$

For the sample used in this study, the material described in Sect. 2.1 was processed into a sample of 20 mm width (W), 100 mm length (L) and 5 mm thickness (t). Fluke 5720A and 5725A were used as current sources and Fluke 8508A was used as a current meter and voltmeter, respectively. After supplying DC 10 A from the current source to electrodes A and B, the supply current was measured with an ammeter, the potential difference (V) was measured with a voltmeter at both ends of the electrodes (C, D), and then the resistance was determined by Ohm's law ($R = V/I$) (Fig. 1). Electrodes C and D were manufactured as knife-edge

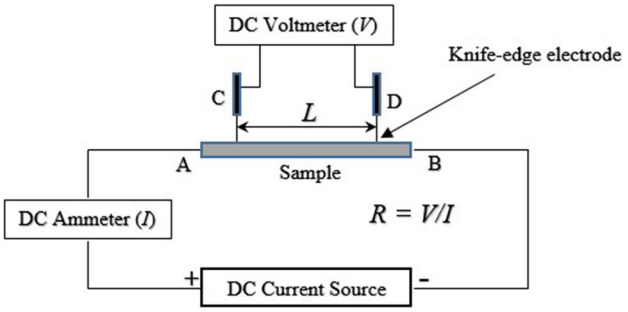

Fig. 1 Configuration diagram of the four-terminal measurement system

electrodes (Fig. 2) to accurately measure the potential difference (V) of the gap (L) between two points of the sample; the voltage was measured after making vertical contact with the sample surface. In addition, for accurate measurement of the thickness and width of the sample, a thickness gauge was manufactured using the measurement principle of a ball-to-ball point contact of two digital micrometers (Fig. 3a and b). The sample thickness was compared and measured using the digital micrometers and a gauge block, the traceability of which was maintained from the national measurement standard. The measurement was performed 9 times at 10 min intervals to obtain an average value and standard deviation of the resistance, and the resistivity and conductivity were calculated using Eqs. (1), (2), and (3). The measurement results are shown in Table 1, and the measurement uncertainty was estimated as shown in Table 2.

2.3 Direct Current Comparator(DCC) Resistance Bridge Method

In this method, two different DC current sources are respectively supplied to two resistors to be compared; one of the current sources is adjusted to equalize the voltage across the two resistors, and the balance is measured with a galvanometer. Simultaneously, the ratio of the current flowing through the two resistors being compared is kept constant through the variable turns N_X (the bridge dial) of the DCC (Fig. 4), until the DC magnetic flux required to obtain a magnetic flux balance between the two circuits generated in the inner core becomes zero. When these two balance conditions are simultaneously satisfied, Eq. (4) is established, and the resistance value (R_X) of the sample to be measured is obtained from the ratio of the DCC resistance bridge dial value and the reference resistance value [4].

$$\frac{N_X}{N_S} = \frac{R_X}{R_S} \tag{4}$$

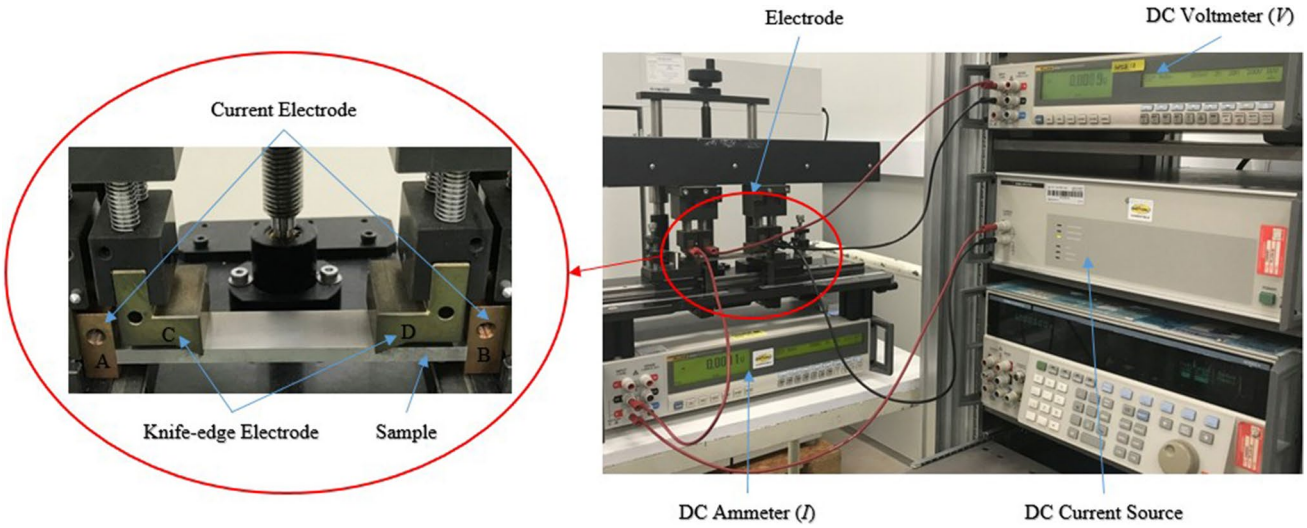

Fig. 2 Photo of the four-terminal measurement system

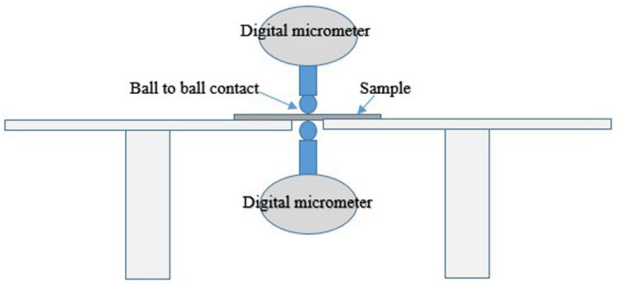

(a) Configuration of the thickness gauge

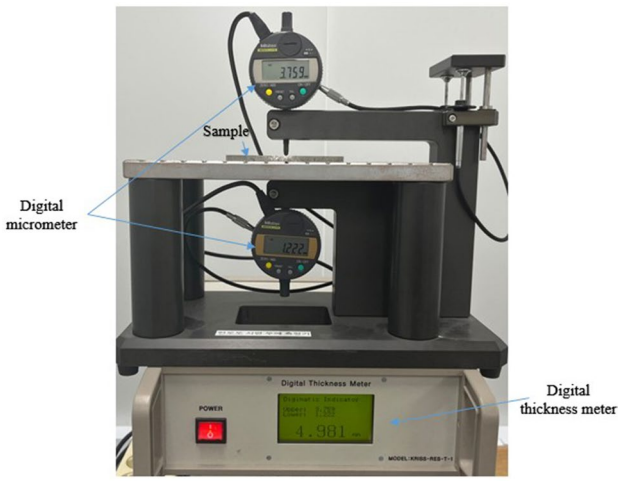

(b) Photo of the thickness gauge

Fig. 3 Thickness gauge

Using a commercial DCC resistance bridge (Model: MI 6010D), composed of the reference resistance R_S and the measurement sample R_X (Fig. 4), the sample R_X was measured using the knife-edge electrodes used in the four-terminal method described in Sect. 2.2, and the resistance was measured to be 725.869 μΩ. The resistivity, conductivity, and conductivity ratio calculated by Eqs. (1), (2), and (3) are shown in Table 3, and the uncertainty evaluation result is shown in Table 4.

The symbols in Fig. 4 are as follows:

N_X: Variable turns of the current comparator, which means dials to measure a resistance.

N_S: Fixed turns of the current comparator, which means reference coils fixed internally.

R_S: Reference resistance for four-terminal measurements.

R_X: Sample resistance for four-terminal measurements.

I_S: Power supply providing a constant current to the reference resistance.

I_P: Power supply providing a constant current to the sample.

D: Detector to sense the voltage difference produced at R_S and R_X.

2.4 Four-Point Probe(FPP) Method

2.4.1 Single Configuration

The single-configuration technique is used to determine sheet resistance by measuring the resistance when contacting a collinear FPP on a sample surface, and then applying the sample size and thickness correction factors against probe spacing [5–7]. Resistance R_S is determined by applying current I_{AD} between the probes A and D and measuring the voltage V_{BC} between the probes B and C (Fig. 5), and is given by Eq. (5).

Table 1 Resistance, resistivity, and conductivity measurement results using the four-terminal resistance measurement method

W(mm)	*t*(mm)	*A*(mm^2)	*L*(mm)	Resistance (μΩ)	Resistivity(ρ) (μΩ·cm)	Conductivity(σ) (kS/cm)	Conductivity ratio (%IACS)
20.02	5.00	100.1	50.98	725.48	142.45	7.020	1.210

Table 2 Measurement uncertainty analysis

Uncertainty factor	Standard uncertainty	Combined standard uncertainty	Expanded uncertainty ($k=2$)
W (mm)	0.05%	0.15%	0.3%
t (mm)	0.08%		
L (mm)	0.05%		
Current source (*I*)	0.005%		
Ammeter (*A*)	0.01%		
Voltmeter (*V*)	0.01%		
Type A	0.01%		

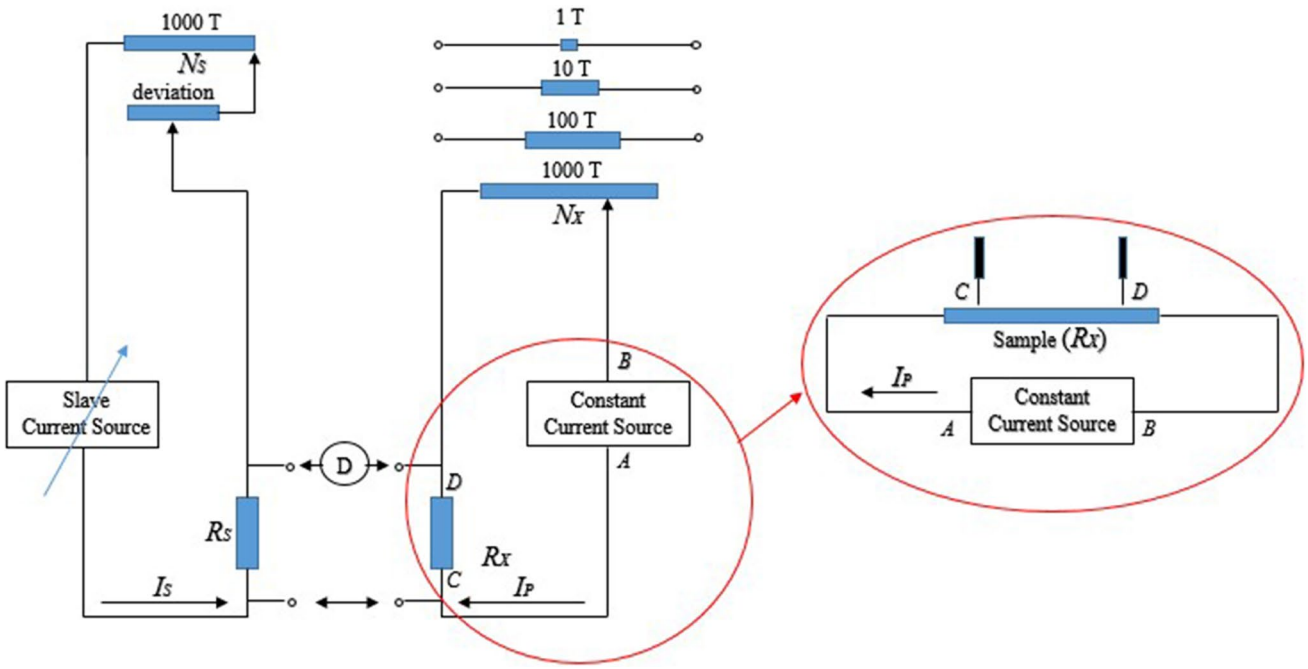

Fig. 4 Schematic diagram of a DCC resistance bridge

Table 3 Measurement results of the resistance, resistivity, conductivity, and conductivity ratio using the DCC resistance bridge

W(mm)	*t*(mm)	*A*(mm^2)	*L*(mm)	Resistance (μΩ)	Resistivity(ρ) (μΩ·cm)	Conductivity(σ) (kS/cm)	Conductivity ratio (%IACS)
20.02	5.00	100.1	50.98	725.87	142.53	7.0163	1.210

$$Rs = V_{BC}/I_{AD}[\Omega] \tag{5}$$

From the resistance, the sheet resistance R_{SS} by the single-configuration technique is given by Eq. (6).

$$R_{SS} = k_S \times R_S\left[\Omega/\text{sq.}\right] \tag{6}$$

where k_S is a correction factor and is given by Eq. (7).

Table 4 Measurement uncertainty evaluation results

Uncertainty factor	Standard uncertainty	Combined standard uncertainty	Expanded uncertainty ($k=2$)
W (mm)	0.05%	0.1%	0.2%
t (mm)	0.07%		
L (mm)	0.05%		
DCC Resistance bridge	0.001%		
Type A	0.02%		

$$k_S = F(W/S) \times F(t/S) \times F(T) \times F(S) \tag{7}$$

From Eq. (7), $F(W/S)$ is a correction factor for sample size W against probe spacing S. The correction factors for the rectangular sample shown in Fig. 5 are summarized in Table 5. In Table 5, $F(W/S)$ is equal to 4.5324 or $\pi/\ln 2$ when W/S is infinite, and it is determined by applying Table 5 for finite W and S [6].

In addition, $F(t/S)$ is the correction factor for sample thickness t against probe spacing S and is shown in Table 6 [7]. The samples used in this study were the same ones used in the above four-terminal resistance measurement method and had the dimensions of $W=20$ mm, $L=100$ mm, $t=5$ mm. The probe spacing of the sheet resistance measuring instrument was 1.00 mm, S was 1.00 mm, and t was 5.00 mm, and therefore, $F(t/S)=0.2753$. $F(T)$ is the temperature correction factor for the measurement environment and if the measurement temperature was (23.0 ± 0.5) °C, the factor equals 1.0 because $F(T)=1-C_T\,(T-23)$. In addition, $F(S)$ is the correction factor for probe spacing and is expressed as $F(S)=1+1.082\times(1-S_2/S)$ in a linear approximation. If S_2 is equal to S, it is equal to 1.000.

2.4.2 Resistivity Measurement

The resistivity is obtained from the following Eq. (8) using the FPP method, and it is given by the product of sheet resistance and thickness.

Table 5 The correction factor for sample size against probe spacing; $F(W/S)$

W/S	$F(W/S)$ of rectangular shape			
	$L/W=1$	$L/W=2$	$L/W=3$	$L/W\geq 4$
1.0	–	–	0.9988	0.9994
1.25	–	–	1.2467	1.2248
1.3	–	1.4788	1.4893	1.4893
1.75	–	1.7196	1.7238	1.7238
2.0	–	1.9454	1.9475	1.9475
2.5	–	2.3532	2.3541	2.3541
3.0	2.4575	2.7000	2.7005	2.7005
4.0	3.1137	3.2246	3.2248	3.2248
5.0	3.5098	3.5749	3.5750	3.5750
7.5	4.0095	4.0361	4.0362	4.0362
10.0	4.2209	4.2357	4.2357	4.2357
15.0	4.3882	4.3947	4.3947	4.3947
20.0	4.4516	4.4553	4.4553	4.4553
40.0	4.5120	4.5129	4.5129	4.5129
∞	4.5324	4.5324	4.5325	4.5321

Table 6 The correction factor for sample thickness against probe spacing; $F(t/S)$

$F(t/S)$	t/S
1.0000	0.100
1.0000	0.141
1.0000	0.200
0.9999	0.333
0.9974	0.500
0.9215	1.000
0.7983	1.414
0.6337	2.000
0.4067	3.333
0.2753	5.000
0.1385	10.00

$$\rho = R_S \times t[\Omega \cdot \mathrm{m}] \tag{8}$$

where ρ is resistivity, R_S is sheet resistance, and t is sample thickness.

The resistivity-measuring device manufactured using this FPP measurement principle is shown in Fig. 6, and when the FPP is brought into contact with the sample surface, the resistivity given from Eq. (8) is indicated on the

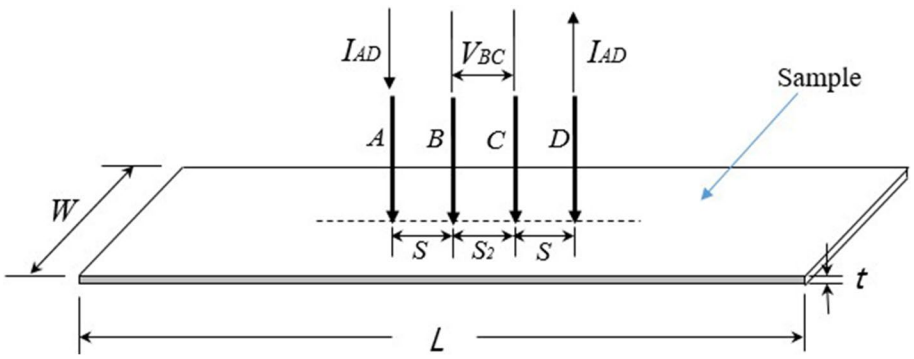

Fig. 5 FPP method and sample of a rectangular shape

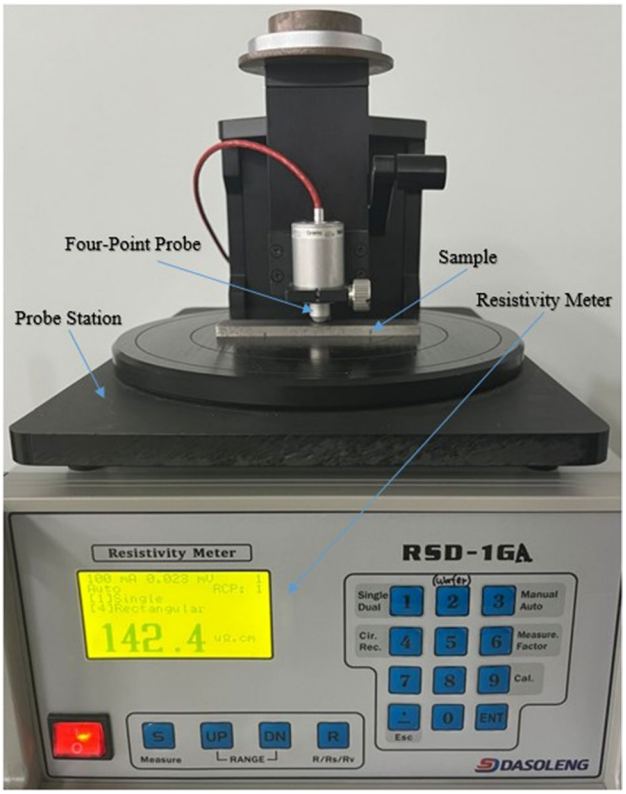

Fig. 6 Resistivity Meter

Table 7 Measurement results for resistivity, conductivity, and conductivity ratio using the FPP method

Resistivity(ρ) (μΩ·cm)	Conductivity(σ) (kS/cm)	Conductivity ratio (%IACS)
142.45	7.020	1.210

window, so it can be easily and conveniently measured. Table 7 shows the resistivity, conductivity, and conductivity ratio measurement results measured with a resistivity meter, and the measurement uncertainty was evaluated with the resistivity meter used for the measurement, probe spacing, and type A, and the evaluation results are shown in Table 8.

2.5 van der Pauw Method

The principle of this method is to construct electrodes at the corners of four points (Fig. 7). For a conductive sample, supply a current in one direction and measure the voltage in the opposite direction to obtain the resistance values of R_A, R_B respectively. From the two values, the resistivity can be determined by Eq. (9) [8].

Table 8 Measurement uncertainty evaluation results

Uncertainty factor	Standard uncertainty	Combined standard uncertainty	Expanded uncertainty ($k=2$)
Resistivity	0.15%	0.2%	0.4%
Probe spacing	0.10%		
Type A	0.02%		

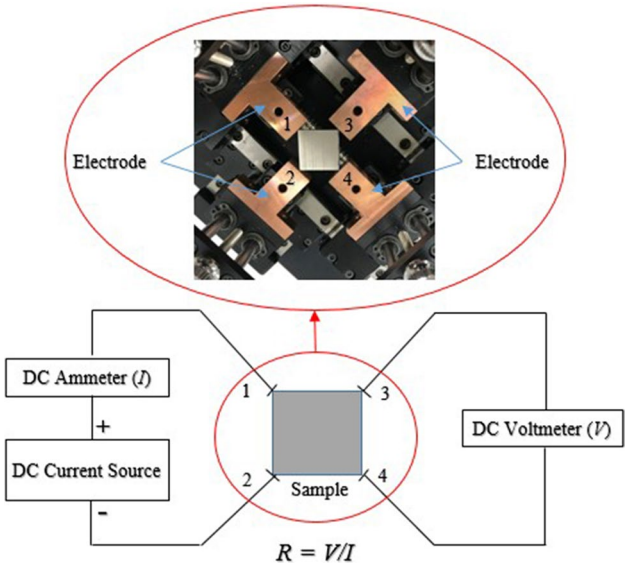

Fig. 7 Configuration for van der Pauw measurement system

$$\rho = \frac{\pi t}{\ln 2}\frac{R_A + R_B}{2} f(r)[\Omega \cdot \mathrm{m}] \tag{9}$$

where ρ is electrical resistivity and t is thickness (mm) of the sample, and $f(r)$ is 1 if the ratio of R_A and R_B is in the range of 1% or less.

The electrical conductivity σ is calculated by Eq. (2), and the electrical conductivity ratio is obtained by Eq. (3). The sample used in this study was the same one used in the above method, and was processed into a square with a size of 20.02 mm × 20.02 mm × 5.00 mm to measure the resistivity by the van der Pauw method.

For measurement, $R_A = V_{34}/I_{12}[\Omega]$ was obtained by building a measurement system as shown in Fig. 7, supplying current to the first and second electrodes of the sample, and measuring the potential difference at the third and fourth electrodes. Then, a current is supplied to the first and third electrodes of the sample, the potential difference is measured at the second and fourth electrode positions to obtain $R_B = V_{24}/I_{13}$ [Ω], the resistivity is obtained from Eq. (9), and the conductivity and conductivity ratio was calculated by the above formulas (2) and

Table 9 Measurement results for the resistivity, conductivity, and conductivity ratio using the van der Pauw method

Resistivity(ρ) (μΩ·cm)	Conductivity(σ) (kS/cm)	Conductivity ratio (%IACS)
142.40	7.022	1.211

(3). The measurement results of the resistivity, conductivity, and conductivity ratio are shown in Table 9, and the measurement uncertainty in Table 10. The current source, ammeter, and voltmeter used for the measurement were the same as the equipment used in the above four-terminal measurement method, and the current was supplied in the forward and reverse directions to reduce the measurement error due to the offset produced during measurements.

2.6 Eddy Current Method

Eddy current is a current of eddy shape generated in a conductor by electromagnetic induction when the magnetic field applied to the conductor changes with time (Fig. 8). That is, using the measurement method using eddy current, the electrical conductivity of the sample was measured using an electrical conductivity meter (Hoking 3000 DL) to which the principle of inducing electromotive force by an alternating magnetic field was applied [9].

This measurement method has a disadvantage in that the measurement accuracy is lowered because of the skin effect of the material and the effect of alternating current. It is, however, the simplest and easiest method for measuring the conductivity of nonmagnetic metals.

The method has the advantage of being able to measure easily because the conductivity is indicated when the probe is placed on a sample with a flat surface (Fig. 9). The conductivity ratio measurement in this study was performed 10 times after calibrating the conductivity meter using a conductivity standard specimen.

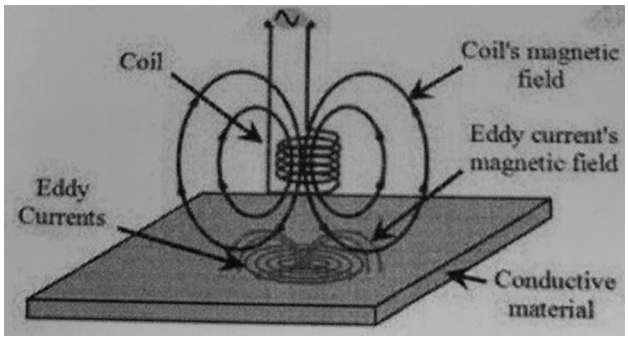

Fig. 8 Eddy current method

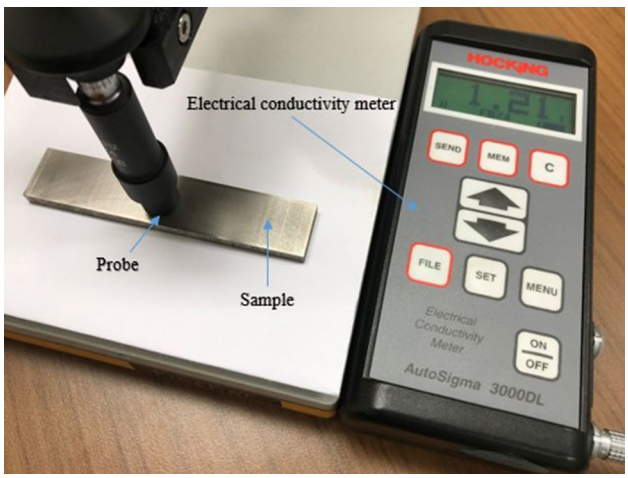

Fig. 9 Eddy current measurement system

3 Summary

There are various methods for evaluating the resistivity, conductivity, and conductivity ratio of conductive materials including metals, but the measurement methods can be applied differently depending on the size, thickness, and shape of the sample. In this study, five measurement methods for conductivity evaluation of the super-alloy single-crystal steel-grade materials used as materials for

Table 10 Measurement uncertainty evaluation results

Uncertainty factor	Standard uncertainty	Combined standard uncertainty	Expanded uncertainty ($k=2$)
W (mm)	0.05%	0.15%	0.30%
t (mm)	0.08%		
L (mm)	0.05%		
Current source (I)	0.005%		
Ammeter (A)	0.01%		
Voltmeter (V)	0.01%		
Type A	0.01%		

Table 11 Results of the resistivity, conductivity, and conductivity ratio using the five measurement methods

	Measurement method	Measured values			Uncertainty ($k=2$) (%)
		resistivity(ρ) (μΩ·cm)	Conductivity (σ) (kS/cm)	Conductivity ratio (% IACS)	
1	4 terminal method	142.45	7.020	1.210	0.3
2	DCC resistance bridge method	142.53	7.016	1.210	0.2
3	FPP method	142.40	7.022	1.211	0.4
4	van der Pauw method	142.40	7.022	1.211	0.3
5	Eddy current method	142.50	7.020	1.210	0.6

high-temperature gas turbine parts were described. The measured results for the resistivity, conductivity, and conductivity ratio are shown in Table 11. The evaluations by all test methods agreed to about 0.1% or less regarding the conductivity. It was confirmed that reliable measurement results can be obtained among the five measurement methods, irrespective of the measurement method selected and depending on the type of sample.

4 Conclusion

Tests of the thermal, mechanical, and electrical properties are required as basic data for building the infrastructure of material property evaluation and a DB for gas turbine core materials. In this study, electrical property tests (resistivity, conductivity, and conductivity ratio) were conducted on H-class superalloy single-crystal steel grades for gas turbine power generation (dimensions: $W=20$ mm, $L=100$ mm, $t=5$ mm). In addition, to confirm the reliability of the measurement results, five measurement methods, namely the four-terminal, DCC resistance bridge, four-point probe, van der Pauw, and eddy current, were compared and evaluated. The comparison showed an agreement of 0.1% or less between the measured values, and the measurement uncertainty [10] was evaluated to be between about 0.2% to 0.6% at the 95% confidence level ($k=2$). In conclusion, this study confirmed that the resistivity, conductivity, and conductivity ratio could be evaluated by various measurement methods depending on the size or shape of the sample; in addition to securing the measurement technology, reliable data were obtained on the electrical properties of superalloy single-crystal steel for gas turbine power generation.

Acknowledgements This research was supported by Korea Institute of Energy Technology Evaluation and Planning(KETEP) grant funded by Ministry of Trade, Industry and Energy(MOTIE) (No. 20181110100410).

References

1. Ministry of Trade, Industry and Energy(MOTIE) (2020.11.30.) Building a gas turbine industry ecosystem that will lead the Green New Deal and carbon-neutral era https://www.motie.go.kr/motie/ne/presse/press2/bbs/bbsView.do?bbs_seq_n=163577&bbs_cd_n=81&currentPage=1&search_key_n=&cate_n=&dept_v=&search_val_v=
2. Kang JH, Yu KM, Lee SH, Nahm SH, Park JY (2022) Precise measurement of electrical conductivity of single-crystal steel grades for high-temperature parts of gas turbines, International Conference on Electrical Facilities and informational technologies 2022 (ICEF 2022), 226–228
3. ASTM B193-78 (1978) Resistivity of electrical conductor materials
4. Mactin MP, Kusters NL (1966) A direct-current comparator ratio bridge for four-terminal resistance measurements. IEEE Trans Instrum Meas 15(4):212–220
5. Smits FM (1958). Measurement of sheet resistivities with the four-point probe, Proceedings of the Institute of Radio Engineers, 711–718
6. ASTM F84: Test method for measuring resistivity of silicon wafers with in-line four-point probe
7. Swartzendruber LJ (1964) Correction factor tables for four-point probe resistivity measurements on thin, circular semiconductor samples, NBS technical note 199
8. van der Pauw LJ (1958) A method of measuring specific resistivity and Hall effect of discs of arbitrary shape. Philips Res Rep 13:1–9
9. Jones AR Sr (1981) Eddy-current characterization of materials and structure, ASTM STP 722, American Society of Testing and Materials, 94–118
10. ISO/IEC (2008) Uncertainty of Measurement—part 3: guide to the expression of uncertainty in measurement (GUM:1995) ISO/IEC Guide 98–3:2008(E)

Jeon-Hong Kang received the M.S. degree in electrical engineering from Hanbat National University, Daejeon, Korea in 1998. He received the Ph.D. degree in electrical engineering from Chungnam National University, Daejeon, Korea, in 2008. From 1987 to present, he is currently working as a Principal Engineer at Center for Electricity and Magnetism of Korea Research Institute of Standards and Science (KRISS). His area of research interest is characteristic evaluation for resistivity of metals, semiconductors and insulators.

Kwang Min Yu received the degree in physics from the Busan National University, Busan, Republic of Korea, in 1983, and the Ph.D. degree from Chungnam National University, Daejeon, Republic of Korea, in 2012. From 1986 to present, he was with the Korea Research Institute of Standards and Science (KRISS), as a Principal Research Scientist. He is responsible for resistance measurement standards. His current main research interests are in high resistance measurements and technology.

Sang Hwa Lee received the B.S. degree in electronics from Hanbat National University, Daejeon, Republic of Korea, in 1994 and the M.S. and Ph.D. degrees in electrical engineering from Chungnam National University, Daejeon, in Republic of Korea, in 2011 and 2019, respectively. From 1985 to present, he was with the Korea Research Institute of Standards and Science (KRISS), Deajeon. He is responsible for ratio measurement standards for direct and alternating-current (ac) high voltage and heavy ac current applications.

Seung Hoon Nahm received his Ph.D. in Mechanical Engineering from Kyungpook National University, Korea in 1997. He is currently working as principal research scientist at the Korea Research Institute of Standard and Science (KRISS). His research interests are the mechanical behavior of materials at the micro and nano scales, hydrogen embrittlement and mechanical behavior of materials at high temperature.

Jae Yeong Park received his Ph.D. in Mechanical Engineering from Pohang University of Science and Technology, Korea in 2018. He is currently working as senior research scientist at the Korea Research Institute of Standard and Science (KRISS). His research interests are the mechanical behavior of materials at high temperature, including anisotropic materials such as gas turbine blades.